Zeolites

DOI: 10.1002/anie.201209638

Formation of Hierarchically Organized Zeolites by Sequential Intergrowth**

*Watcharop Chaikittisilp, Yuki Suzuki, Rino R. Mukti, Tatsuya Suzuki, Keisuke Sugita, Keiji Itabashi, Atsushi Shimojima, and Tatsuya Okubo**

Hierarchically organized porous materials can provide multidimensional spatial networks on different length scales with improved characteristics relevant to molecular diffusion.[1] Zeolites that are microporous crystalline materials having pores and channels at molecular dimensions are of great importance for industrial applications.[2] However, the presence of only micropores in zeolite frameworks often limits the molecular diffusion and therefore, restricts the transport of bulky molecules. This problem can be resolved by shortening the effective diffusion path lengths, which has been achieved by miniaturizing zeolite crystals,[3] delaminating or exfoliating layered zeolites,[4] synthesizing zeolite nanosheets,[5] and introducing mesopores into zeolite particles.[6–12] Among these solutions, the fabrication of hierarchical zeolites with micro- and mesoporosity is of interest because it combines intrinsic micropores with bypass-interconnected mesopores, and therefore, enhances both the micropore accessibility and molecular traffic within zeolite particles.[1,7b,12]

Hierarchical zeolites have been produced using several techniques, including top-down desilication by alkali post-synthetic treatment[6] and bottom-up directed assembly by hard[7] or soft[8–11] templates. The hard-template method requires multistep procedures and is therefore unfavorable for large-scale production. Alternatively, the direct introduction of organic mesopore-generating agents (mesoporogens) during zeolite synthesis can create uniform mesopores. The use of such mesoporogens is currently one of the most promising methods for the single-step construction of hierarchical zeolites. Progress has been made using well-designed mesoporogens composed of long hydrophobic chains and hydrophilic zeolitic structure-directing groups to generate zeolites with tunable mesoporosity[9a,10] and to direct the hierarchical assembly of zeolite nanosheets, yielding mesoporous zeolites with house-of-cards-like structures.[5a,9c,11] These hierarchical nanosheets showed excellent catalytic performance in several important reactions because the presence of thin layers with specific crystalline faces facilitates catalysis at the exteriors or pore mouths.[13] Such mesoporogens are probably necessary for the direct, single-step synthesis of hierarchical zeolites.

Herein we report an alternative, mesoporogen-free approach for the construction of hierarchically organized MFI zeolites by sequential intergrowth using a simple organic structure-directing agent (OSDA). The selection of an appropriate OSDA and optimized synthesis conditions that can form plate-like zeolites with enhanced 90° rotational intergrowths seems to be a key to achieving a hierarchical structure with three classes of porosity in one structure: the intrinsic microporosity of the zeolite framework together with mesoporosity existing within the zeolite plates and macroporosity stemming from the complex intergrown structure.

Epitaxial and rotational intergrowths are commonly observed in many zeolites.[14] We have hypothesized that by engineering the zeolite intergrowths, hierarchically organized zeolites can be constructed without the need for mesoporogens. In particular, we have focused on the MFI zeolite because it is an excellent catalyst in many industrial processes[2b,15] and a promising material for membrane separation.[1b] MFI zeolite that contains sinusoidal channels along the *a* axis interconnected with straight channels along the *b* axis is often formed with 90° rotational intergrowths, in which substantial (*h*00) faces are epitaxially overgrown on the (0*k*0)

[*] Dr. W. Chaikittisilp,[$] [+] Y. Suzuki,[#] [+] Dr. R. R. Mukti,[++]
Dr. K. Itabashi, Prof. Dr. A. Shimojima, Prof. Dr. T. Okubo
Department of Chemical System Engineering
The University of Tokyo
7-3-1 Hongo, Bunkyo-ku, Tokyo 113-8656 (Japan)
E-mail: okubo@chemsys.t.u-tokyo.ac.jp
Homepage: http://www.zeolite.t.u-tokyo.ac.jp
Dr. T. Suzuki, Dr. K. Sugita
Basic Chemicals Research Laboratory
Sumitomo Chemical Co. Ltd.
5-1 Sobiraki-cho, Niihama, Ehime 792-8521 (Japan)

[++] Present address: Division of Inorganic and Physical Chemistry, Institut Teknologi Bandung
Jl. Ganesha no. 10, Bandung 40132 (Indonesia)

[$] Present address: World Premier International (WPI) Research Center for Materials Nanoarchitectonics (MANA), National Institute for Materials Science
1-1 Namiki, Tsukuba, Ibaraki 305-0044 (Japan)

[#] Present address: Technical Research & Development Bureau
Nippon Steel & Sumitomo Metal Corporation
20-1 Shintomi, Futtsu, Chiba 293-8511 (Japan)

[+] These authors contributed equally to this work.

[**] This study was supported in part by Sumitomo Chemical Co. Ltd., a Grant-in-Aid for Scientific Research (B) from the Japan Society for the Promotion of Science (JSPS), and a Global COE Program (Mechanical Systems Innovation) from the Ministry of Education, Culture, Sports, Science and Technology (MEXT) (Japan). W.C. thanks MEXT for a Monbukagakusho Scholarship. R.R.M. thanks JSPS for a postdoctoral fellowship. We are grateful to Dr. Yoshihiro Kamimura for his assistance with the solid-state NMR measurements.

Supporting information for this article is available on the WWW under http://dx.doi.org/10.1002/anie.201209638.

faces.[14a,16] The tetrapropylammonium (TPA) cation is the most common and probably the most energetically favored OSDA for MFI zeolite formation.[17] TPA cations are situated at the intersection of the straight and sinusoidal channels. Therefore, we have considered that organic molecules with slight differences from TPA molecules could still direct the crystallization of MFI zeolites but could also enhance the formation of 90° rotational intergrowths. Very recently, in a similar strategy, self-pillared zeolite nanosheets containing micro- and mesoporosity were synthesized by repetitive branching using tetrabutylphosphonium cations as an OSDA.[12] Although the hierarchical zeolites could be obtained without the use of mesoporogens, the use of a phosphonium-based OSDA would affect the physicochemical properties of the resultant zeolites because the decomposition of the OSDA by conventional thermal calcination cannot totally remove phosphorus from the zeolite structure, and therefore, a certain amount of phosphorus debris may remain in the zeolites.

Among the many OSDAs for MFI zeolite, we have focused herein on dimers of the TPA cation, $(C_3H_7)_3N^+$-$(CH_2)_nN^+(C_3H_7)_3$, because such diquaternary ammonium cations with $n = 5$–7 are situated in the framework with the N-N chains being better fitted along the straight channels than along the sinusoidal channels.[18] This limits the degree of molecular motion within the framework, particularly in the case of OSDAs with shorter alkyl-chain spacers. The TPA dimer with $n = 5$, hereafter denoted as diquat-C5, possesses an intramolecular N-N distance of 0.7 nm, which is much shorter than the distances between two intersections along the straight (1.0 nm) and sinusoidal (1.2 nm) channels. Although previous molecular mechanics simulations suggested that diquat-C5 is not readily accommodated in the zeolite channels, it can still direct the formation of MFI zeolites.[18a,c] Accordingly, the diquat-C5 cations have to adapt their intramolecular N-N distance to be occluded intact within the MFI framework, perhaps along the straight channel, generating structural constraints or stresses, and thereby yielding framework distortion, as suggested by synchrotron X-ray analyses.[18c] This event limits crystal growth along the *b* axis, resulting in an MFI zeolite with a plate-like morphology but with a few intergrowths.[18c] To generate hierarchical zeolites composed of such plate-like crystals, zeolites should be synthesized under conditions with more pronounced surface nucleation. In a previous report,[18c] zeolites were synthesized from very dilute solutions in the presence of seed crystals, thus limiting the formation of intergrowths. Although a non-seeded synthesis was also carried out, the formation of intergrowths was inhibited because the diquat-C5 partially decomposed under the synthetic conditions.

Field-emission scanning electron microscopy (FE-SEM) and secondary electron (SE) images of the product obtained after hydrothermal synthesis at 130 °C for 264 hours are shown in Figure 1 a,b, respectively (see experimental details in the Supporting Information). The powder X-ray diffraction (XRD) pattern (Figure 2 a) confirms that the obtained product possesses the MFI zeolite structure. These siliceous MFI (silicalite-1) zeolite crystals have an unusual intergrown organization because of the 90° rotation of the adjoining

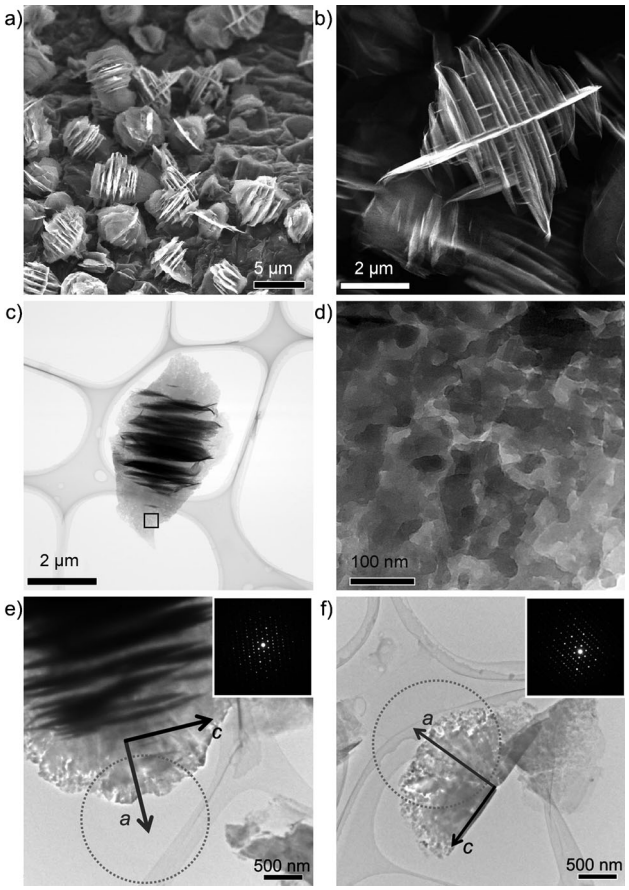

Figure 1. a) FE-SEM, b) SE, c,d) BF-STEM, and e,f) TEM images of silicalite-1 zeolites synthesized at 130 °C for 264 h. The rough background in (a) is carbon paste used for sample preparation. The square area in (c) is shown as a magnified image in (d). Insets in (e,f) are SAED patterns taken from the circled regions in the corresponding TEM images.

faces. To the best of our knowledge, this is the first observation of such a complex morphology for an MFI zeolite. The bright-field scanning transmission electron microscopy (BF-STEM) images reveal that the zeolite plates are probably constructed by the aggregation of nanoparticles (Figure 1 c,d). The dot patterns of selected-area electron diffraction (SAED) of both the main plate (Figure 1 e) and the crystal flake (Figure 1 f) indicate single-crystalline materials. In addition, both SAED patterns reveal that the crystals are viewed along the [010] zone axis, suggesting that the *b* axis (i.e., the straight channels) runs perpendicular to the surface of each crystal plate.

To obtain further insights into the organization process, the textural evolution of the obtained silicalite-1 crystals was investigated, as shown in Figure 2. The first visible Bragg diffraction appears after 135 hours of crystallization (see Figure 2 a). Before the onset of crystallization, the FE-SEM image shows that the products are nanoparticle aggregates (Figure 2 b). No crystal-like, faceted particles were observed at this stage, consistent with the corresponding XRD pattern. After 135 hours (Figure 2 c), the plate-like particles were first seen together with the nanoparticle aggregates. These plate-like particles were probably silicalite-1 crystals, as suggested

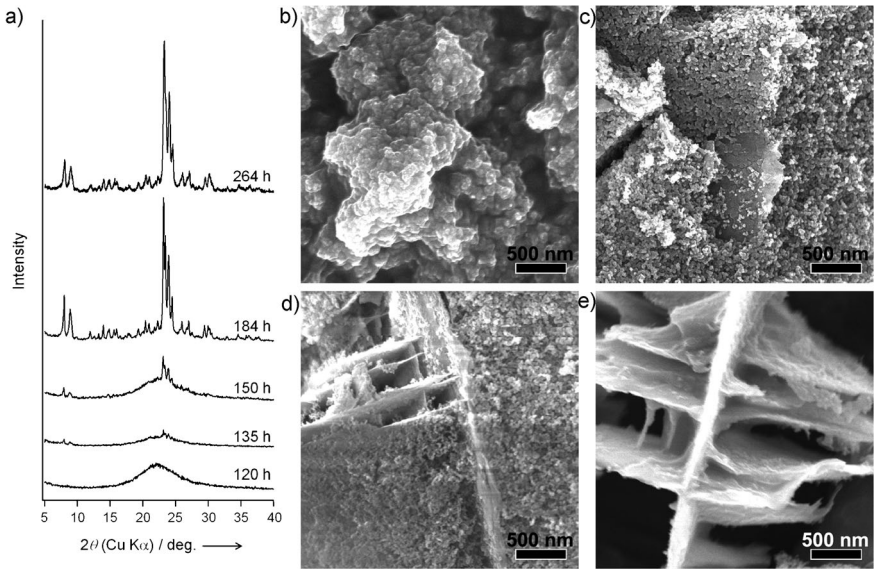

Figure 2. a) Powder XRD patterns of the products obtained at 130 °C after 120–264 h. FE-SEM images of the products after reaction times of b) 120 h, c) 135 h, d) 150 h, and e) 184 h.

by the XRD pattern. The unusual intergrown structure developed gradually during the course of crystallization (Figure 2 d,e).

The calcined products synthesized at 130 °C for 150 hours were further characterized by TEM. The SAED patterns of representative regions of the nanoparticle aggregates are shown in the insets of Figure 3 a and Figure S1 a, confirming that the resulting nanoparticles are amorphous. High-resolution TEM (HR-TEM) images (Figure 3 b; Figure S1 b) further supported the amorphous nature of these nanoparticles. As expected, in contrast, plate-like particles exhibited SAED patterns common to MFI zeolite (Figure 3 c; Figure S1 c; insets). Lattice fringes indicative of crystalline orders were clearly observed in the HR-TEM images (Figure 3 d; Figure S1 d), corroborating that the plate-like particles are silicalite-1 zeolites.

A scheme of the formation of hierarchically organized MFI zeolites based on the above results is shown in Figure 4. In the early stage of crystallization, the amorphous nanoparticles, probably hydrated diquat-C5-silica composites, are formed. These composite nanoparticles aggregate to form very thin MFI zeolite plates. Although the formation process is still unclear, viable zeolite nuclei may be formed by the oriented-aggregation mechanism, the solid-state-like disorder-to-order transformation, reorganization at the solid-liquid interface, or a combination thereof.[19] Under the present synthesis conditions, the 90° rotational intergrowths are enhanced and developed during the crystal growth process. The intergrown crystal flakes are also made of nanoparticle aggregates. The composite nanoparticles and the soluble species together supply the precursors for crystal growth, and subsequently, zeolite crystals evolve into the hierarchical structure.

We considered that increasing the synthesis temperature could enhance the crystal intergrowth,[16] thereby enhancing the formation of the hierarchical structures. Therefore, silicalite-1 zeolites were also synthesized at 150 °C and 175 °C. Clearly, the hierarchical structure is more pronounced after synthesis at 150 °C, as shown in Figure 5 a–c. The powder

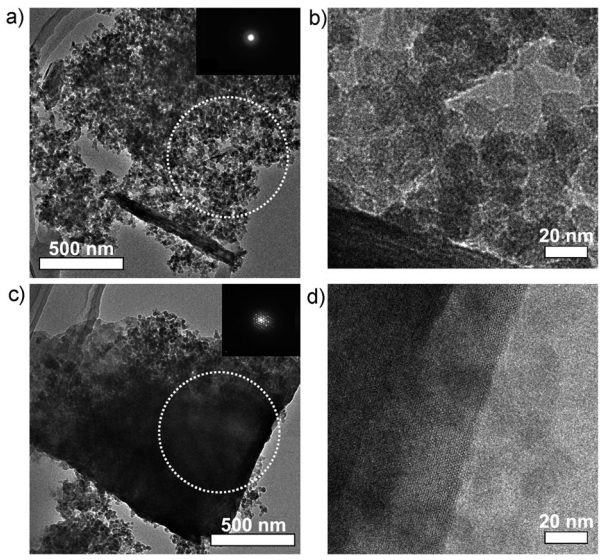

Figure 3. a,c) TEM and b,d) HR-TEM images of the calcined products synthesized at 130 °C for 150 h. HR-TEM images in (b,d) correspond to those in (a,c), respectively. Insets in (a,c) show the corresponding SAED patterns taken from the circled areas.

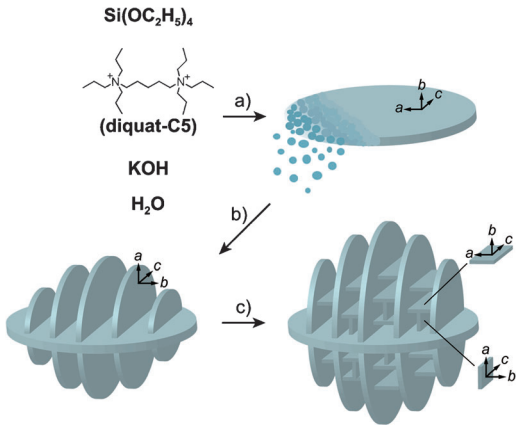

Figure 4. Schematic representation of the formation of hierarchically organized MFI zeolite. a) Amorphous nanoparticles, probably hydrated diquat-C5–silica composites, form from a solution. These nanoparticles aggregate to form MFI zeolite plates. b) The 90° rotational intergrowths develop during crystal growth, in which each intergrown crystal flask also forms from nanoparticle aggregates. c) The nanoparticles and the soluble species in solution together supply the precursors for crystal growth, and finally, zeolite crystals evolve into the hierarchical structure.

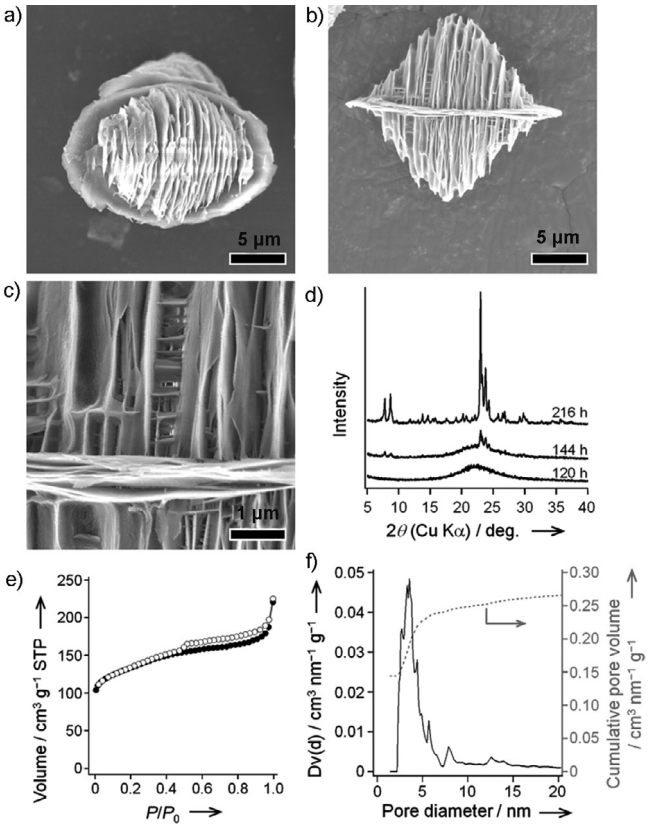

Figure 5. a–c) FE-SEM images of the products obtained after crystallization at 150 °C for 216 h. d) Powder XRD patterns of the products obtained after 120–216 h. e) Nitrogen adsorption (●)-desorption (○) isotherms and f) corresponding NL-DFT pore size distribution and cumulative pore volume of the calcined product after crystallization for 216 h.

XRD patterns (Figure 5 d) confirmed that the products are MFI zeolite. Interestingly, plate-like silicalite-1 zeolites with less-intergrown structures were obtained when the synthesis temperature was further raised to 175 °C (Figure S2). We speculate that Ostwald's law of successive reactions is, at least in part, responsible for the formation of the less-intergrown silicalite-1 at 175 °C. This law essentially describes the consumption of the less-stable phase, the subsequent formation of a thermodynamically more stable phase, and so on, until the most stable phase is formed.[17] At 175 °C, such successive ripening proceeds rapidly, and therefore, the resulting zeolites did not form the hierarchical structure. Observation of such less-intergrown silicalite-1 synthesized at 130 °C and 150 °C after prolonged reaction times (Figure S3) additionally supported the theory of Ostwald ripening. These results also suggest that the obtained silicalite-1 was the result of a kinetically controlled synthetic pathway.

As is well known, quaternary ammonium cations can undergo a Hofmann elimination, particularly at high temperature. The solid-state ^{1}H-^{13}C cross-polarization magic-angle spinning (CP/MAS) NMR spectrum of the silicalite-1 synthesized at 150 °C reveals that the diquat-C5 cations are occluded intact in the zeolite product (Figure S4). In contrast, the product synthesized at 175 °C showed additional signals, probably arising from Hofmann elimination products. For example, the signals at $\delta \approx 30$, 118, and 137 ppm can be assigned to the center carbon of 1,4-pentadiene, the β-olefinic carbon ($CH_2\boldsymbol{C}H{=}CH_2$), and the α-olefinic carbon ($CH_2CH{=}\boldsymbol{C}H_2$), respectively. This partial decomposition of the diquat-C5 SDA seems to affect the morphology of the resulting zeolite products,[18b,c] in addition to Ostwald's ripening.

Nitrogen sorption isotherms of the silicalite-1 sample show a large uptake at low relative pressures, a hysteresis loop at moderate relative pressures, and a slight uptake at higher relative pressures, indicating the presence of micro-, meso-, and macroporosity, respectively (Figure 5 e). The apparent specific Brunauer–Emmett–Teller (BET) surface area and the total pore volume (at $P/P_o = 0.99$) were calculated to be 490 $m^2 g^{-1}$ and 0.35 $cm^3 g^{-1}$, respectively. The external surface area and micropore volume were estimated by the *t*-plot method to be 215 $m^2 g^{-1}$ and 0.11 $cm^3 g^{-1}$, respectively. The pore-size distribution and cumulative pore volume calculated by non-local density functional theory (NL-DFT) are depicted in Figure 5 f. The pore-size distribution was relatively narrow with a diameter centered at 3.3 nm. The SEM, TEM, and nitrogen physisorption results indicate that the silicalite-1 zeolite possessed the intrinsic microporosity of a zeolite framework together with mesoporosity within the zeolite plates and macroporosity stemming from the complex intergrown structure.

We also explored the synthesis of aluminosilicate MFI (ZSM-5) by adding an aluminum source to the starting synthesis solution at different Si/Al ratios. The powder XRD patterns confirmed the formation of MFI zeolite (Figure S5 a). The obtained ZSM-5 zeolites showed a similar morphology, indicating that the presence of Al did not inhibit the formation of this unique structure (Figure S5 c,d). Solid-state ^{27}Al MAS NMR spectra of the calcined samples (Figure S5 b) suggested that Al atoms are located at the tetrahedral positions of the framework, although non-framework, octahedral Al species also appear. The nitrogen sorption isotherms in Figure S6 a show that the obtained ZSM-5 also possesses micro-, meso-, and macroporosity. NL-DFT analyses confirmed the presence of mesoporosity (Figure S6 b), although the mesopore size distributions were less uniform than that of the silicalite-1 counterpart (see above). These hierarchical ZSM-5 zeolites are potentially promising for the catalytic conversion of bulky molecules and biomass processing. Such topics are vital and merit a detailed investigation in future studies.

In summary, we have demonstrated a new approach for the construction of hierarchically organized zeolites by sequential intergrowth. For the first time, a complex and unusual morphology was observed for MFI zeolites. These zeolites possessing micro-, meso-, and macroporosity have been produced by a simple, single-step, hydrothermal synthesis using a small OSDA without meso- or macroporogens. The use of an OSDA that is imperfectly fitted to the zeolite framework, yet can direct its formation, is thought to be responsible for the formation of very thin zeolite plates with enhanced 90° rotational intergrowth, thereby for the construction of hierarchically organized structure. This concept would be applicable to other zeolite frameworks and related

porous crystalline materials that can form such rotational intergrowths.

Received: December 2, 2012
Published online: February 18, 2013

Keywords: crystal growth · hierarchical organization · mesoporous materials · structure-directing agents · zeolites

[1] a) M. Hartmann, *Angew. Chem.* **2004**, *116*, 6004 – 6006; *Angew. Chem. Int. Ed.* **2004**, *43*, 5880 – 5882; b) M. A. Snyder, M. Tsapatsis, *Angew. Chem.* **2007**, *119*, 7704 – 7717; *Angew. Chem. Int. Ed.* **2007**, *46*, 7560 – 7573; c) J. Pérez-Ramírez, C. H. Christensen, K. Egeblad, C. H. Christensen, J. C. Groen, *Chem. Soc. Rev.* **2008**, *37*, 2530 – 2542.

[2] a) M. E. Davis, *Nature* **2002**, *417*, 813 – 821; b) A. Corma, *Chem. Rev.* **1997**, *97*, 2373 – 2420.

[3] L. Tosheva, V. P. Valtchev, *Chem. Mater.* **2005**, *17*, 2494 – 2513.

[4] a) A. Corma, V. Fornes, S. B. Pergher, Th. L. M. Maesen, J. G. Buglass, *Nature* **1998**, *396*, 353 – 356; b) S. Maheshwari, E. Jordan, S. Kumar, F. S. Bates, R. L. Penn, D. F. Shantz, M. Tsapatsis, *J. Am. Chem. Soc.* **2008**, *130*, 1507 – 1516.

[5] a) M. Choi, K. Na, J. Kim, Y. Sakamoto, O. Terasaki, R. Ryoo, *Nature* **2009**, *461*, 246 – 249; b) W. Park, D. Yu, K. Na, K. E. Jelfs, B. Slater, Y. Sakamoto, R. Ryoo, *Chem. Mater.* **2011**, *23*, 5131 – 5137.

[6] a) M. Ogura, *Catal. Surv. Asia* **2008**, *12*, 16 – 27; b) M. Ogura, S. Shinomiya, J. Tateno, Y. Nara, E. Kikuchi, M. Matsukata, *Chem. Lett.* **2000**, 882 – 883; c) J. C. Groen, L. A. A. Peffer, J. A. Moulijn, J. Pérez-Ramírez, *Chem. Eur. J.* **2005**, *11*, 4983 – 4994; d) D. Verboekend, S. Mitchell, M. Milina, J. C. Groen, J. Pérez-Ramírez, *J. Phys. Chem. C* **2011**, *115*, 14193 – 14203.

[7] a) W. Fan, M. A. Snyder, S. Kumar, P.-S. Lee, W. C. Yoo, A. V. McCormick, R. L. Penn, A. Stein, M. Tsapatsis, *Nat. Mater.* **2008**, *7*, 984 – 991; b) H. Chen, J. Wydra, X. Zhang, P.-S. Lee, Z. Wang, W. Fan, M. Tsapatsis, *J. Am. Chem. Soc.* **2011**, *133*, 12390 – 12393; c) S.-S. Kim, J. Shah, T. J. Pinnavaia, *Chem. Mater.* **2003**, *15*, 1664 – 1668.

[8] a) F.-S. Xiao, L. Wang, C. Yin, K. Lin, Y. Di, J. Li, R. Xu, D. S. Su, R. Schlögl, T. Yokoi, T. Tatsumi, *Angew. Chem.* **2006**, *118*, 3162 – 3165; *Angew. Chem. Int. Ed.* **2006**, *45*, 3090 – 3093; b) H. Wang, T. J. Pinnavaia, *Angew. Chem.* **2006**, *118*, 7765 – 7768; *Angew. Chem. Int. Ed.* **2006**, *45*, 7603 – 7606.

[9] a) M. Choi, H. S. Cho, R. Srivastava, C. Venkatesan, D.-H. Choi, R. Ryoo, *Nat. Mater.* **2006**, *5*, 718 – 723; b) K. Na, M. Choi, W. Park, Y. Sakamoto, O. Terasaki, R. Ryoo, *J. Am. Chem. Soc.* **2010**, *132*, 4169 – 4177; c) K. Na, W. Park, Y. Seo, R. Ryoo, *Chem. Mater.* **2011**, *23*, 1273 – 1279.

[10] R. R. Mukti, H. Hirahara, A. Sugawara, A. Shimojima, T. Okubo, *Langmuir* **2010**, *26*, 2731 – 2735.

[11] A. Inayat, I. Knoke, E. Spiecker, W. Schwieger, *Angew. Chem.* **2012**, *124*, 1998 – 2002; *Angew. Chem. Int. Ed.* **2012**, *51*, 1962 – 1965.

[12] X. Zhang, D. Liu, D. Xu, S. Asahina, K. A. Cychosz, K. V. Agrawal, Y. A. Wahedi, A. Bhan, S. A. Hashimi, O. Terasaki, M. Thommes, M. Tsapatsis, *Science* **2012**, *336*, 1684 – 1687.

[13] A. Corma, *Nature* **2009**, *461*, 182 – 183.

[14] a) E. Stavitski, M. R. Drury, D. A. M. de Winter, M. H. F. Kox, B. M. Weckhuysen, *Angew. Chem.* **2008**, *120*, 5719 – 5722; *Angew. Chem. Int. Ed.* **2008**, *47*, 5637 – 5640; b) J. M. Newsam, M. M. J. Treacy, W. T. Koetsier, C. B. de Gruyter, *Proc. R. Soc. London Ser. A* **1988**, *420*, 375 – 405; c) G. R. Millward, S. Ramdas, J. M. Thomas, M. T. Barlow, *J. Chem. Soc. Faraday Trans. 2* **1983**, *79*, 1075 – 1082; d) M. M. J. Treacy, D. E. W. Vaughan, K. G. Strohmaier, J. M. Newsam, *Proc. R. Soc. London Ser. A* **1996**, *452*, 813 – 840; e) T. Okubo, T. Wakihara, J. Plévert, S. Nair, M. Tsapatsis, Y. Ogawa, H. Komiyama, M. Yoshimura, M. E. Davis, *Angew. Chem.* **2001**, *113*, 1103 – 1105; *Angew. Chem. Int. Ed.* **2001**, *40*, 1069 – 1071; f) T. Wakihara, S. Yamakita, K. Iezumi, T. Okubo, *J. Am. Chem. Soc.* **2003**, *125*, 12388 – 12389.

[15] Y. Izumi, H. Ichihashi, Y. Shimazu, M. Kitamura, H. Sato, *Bull. Chem. Soc. Jpn.* **2007**, *80*, 1280 – 1287.

[16] a) T. Nakazawa, M. Sadakata, T. Okubo, *Microporous Mesoporous Mater.* **1998**, *21*, 325 – 332; b) W. Chaikittisilp, M. E. Davis, T. Okubo, *Chem. Mater.* **2007**, *19*, 4120 – 4122.

[17] M. E. Davis, R. F. Lobo, *Chem. Mater.* **1992**, *4*, 756 – 768.

[18] a) E. de Vos Burchart, J. C. Jansen, B. van de Graaf, H. van Bekkum, *Zeolites* **1993**, *13*, 216 – 221; b) L. W. Beck, M. E. Davis, *Microporous Mesoporous Mater.* **1998**, *22*, 107 – 114; c) G. Bonilla, I. Díaz, M. Tsapatsis, H.-K. Jeong, Y. Lee, D. G. Vlachos, *Chem. Mater.* **2004**, *16*, 5697 – 5705.

[19] a) T. M. Davis, T. O. Drews, H. Ramanan, C. He, J. Dong, H. Schnablegger, M. A. Katsoulakis, E. Kokkoli, A. V. McCormick, R. L. Penn, M. Tsapatsis, *Nat. Mater.* **2006**, *5*, 400 – 408; b) W. Fan, M. Ogura, G. Sankar, T. Okubo, *Chem. Mater.* **2007**, *19*, 1906 – 1917; c) V. P. Valtchev, K. N. Bozhilov, *J. Am. Chem. Soc.* **2005**, *127*, 16171 – 16177.

